Optimal Induced Spreading of SIS Epidemics in Networks

Zhidong He, and Piet Van Mieghem, *Member, IEEE*

***Abstract*— Induced spreading aims to maximize the infection probabilities of some target nodes by adjusting the nodal infection rates, which can be applied in biochemical and information spreading. We assume that the adjustment of the nodal infection rates has an associated cost and formulate the induced spreading for SIS epidemics in networks as an optimization problem under a constraint on total cost. We address and solve both a static model and a dynamic model for the optimization of the induced SIS spreading. By numerical results in some artificial and real networks, we investigate the effect of the network topology on the optimal induced strategy with a quadratic cost function. In the static method, the infection rate increment on each node is coupled to both the degree and the average hops to the targets. In the dynamic method, we show that the effective resistance could be a good metric to indicate the minimum total cost for targeting a single node. We also illustrate that the minimum total cost increases much more slowly with the increasing fraction of targets in the SIS model than in linear control systems.**

***Index Terms*— Virus spread; Network topology; Network analysis and control**

I. Introduction

SINCE the earliest account of mathematical modeling of diseases was proposed by Daniel Bernoulli in 1766, epidemic models help us to better understand dynamics of spreading processes [1]. Spreading in networks can describe many physical phenomena and human activities, such as information spreading on social networks, biological diseases [2] and computer viruses on cyber-physical networks [3]. Some previous research investigated the strategies to eliminate or control the spreading of viruses as quickly as possible [4]. The optimal epidemics control problem for mean-field models can be converted into a spectral control problem, e.g., how to decrease the spectral radius of a graph [5] more efficiently by some strategies (e.g., link removals)? Preciado *et al.* [6] propose the budget-constrained allocation problem and present a solution framework based on Geometric Programming to control the epidemics by adjusting the infection rates and the curing rates of nodes.

Although the existing work on controlling the spreading has presented some useful proposals and frameworks on a microscopic level, the previous research focuses on the performance of the whole network. Induced spreading or targeted spreading is a more general task, which aims to maximize (minimize) the infection probability of some specific nodes instead of all nodes in the network. The induced spreading problem is first introduced by Sun *et al.* [7] for identifying the single best spreader if the spreading only aims to cover a specific group of nodes. The induced spreading problem is inspired by many real applications. In the biochemical application, induced spreading can be applied for targeting biochemical cascades to treat cancer [8]. We prefer to guide the drug to reach affected areas effectively with a minimum dose to reduce side effects. In the context of information spreading, some advertisements (e.g., cigarettes) on the Internet should reach as much as possible to the potential customs; and a strategy for active cyber defense [9] based on spreading patches for targeting the infected computers should be designed.

Notwithstanding the importance of the induced spreading, the methods and properties of the induced spreading have been considered only in a few works [7] [10]. In this paper, we focus on the Susceptible-Infected-Susceptible (SIS) model and specialize in the optimal induced spreading problem in networks. We address two optimization models: the static and the dynamic. The static optimization aims to maximize the sum of the steady-state infection probabilities of the target nodes, under a constraint on the nodal infection rates. In the dynamic optimization, we model the induced spreading as an optimal control problem for maximizing the cumulative infection probabilities of the target nodes in a time interval, where the time-dependent nodal infection rates are the control variables. For the dynamic optimization, Lokhov and Saad [10] propose a framework for maximizing impact in spreading processes based a message-passing [11] under the assumption of a locally tree-like network. Instead, we formulate both optimization problems based on the heterogeneous NIMFA model [12] [13] for better investigating the effect of topology on the induced spreading behaviors.

We solve the static optimization problem by the Differential Evolution algorithm [14], and solve the dynamic optimization based on the optimality system. Further, we investigate the impact of the topological properties of the target nodes on the induced strategy by numerical results in some artificial and real networks. We explore the behaviors of both the static and dynamic induced spreading, as well as compare the performance between these two optimization models.

This paper is organized as follows. Section 2 briefly introduces the SIS model in networks and the heterogeneous NIMFA model. We propose and solve the static optimization for the induced spreading in Section 3, and address the

The authors are with Faculty of Electrical Engineering, Mathematics and Computer Science, Delft University of Technology, P.O Box 5031, 2600 GA Delft, The Netherlands (e-mail: {Z.He, P.F.A.VanMieghem}@tudelft.nl).

dynamic optimization for the induced spreading in Section 4. In Section 5, we explore some properties of the induced strategy by numerical results. We introduce the related work in Section 6 and conclude this paper in Section 7.

II. Preliminaries and Model

A. SIS model in networks

The SIS model is an epidemic model where each infected item can be cured, and becomes susceptible again after recovering from the disease [15]. We define a Bernoulli random variable $X_i(t) \in \{0,1\}$ as the state of a node i at time t, with $X_i(t)=0$ for the healthy state and $X_i(t)=1$ for the infected state. The network G with N nodes and L links is represented by an adjacent matrix A, where $a_{ij}=1$ if there is a link between node i and node j, otherwise $a_{ij}=0$. We denote by $\mathcal{N}=\{1,2,\ldots,N\}$ the set of nodes in the network.

In Markovian Susceptible-Infected-Susceptible (SIS) epidemics, both the curing and infection processes are Poisson processes [15]. Since X_i is a Bernoulli random variable, it holds that $E[X_i(t)] = \Pr[X_i(t)=1]$, and the exact SIS governing equation for node i equals

$$\frac{dE[X_i(t)]}{dt} = E\left[-\delta X_i(t) + \beta(1-X_i(t))\sum_{k=1}^{N} a_{ki}X_k(t)\right] \quad (1)$$

The ratio between the infection rate β and the curing rate δ is called the effective infection rate $\tau=\beta/\delta$. The SIS model features a phase transition [16] [17] around the epidemic threshold τ_c. Viruses with an effective infection rate τ above the epidemic threshold τ_c can infect a sizeable portion of the population on average and stay for a long time in the network. This long period is called the metastable state [18].

B. Heterogeneous NIMFA model

In the N-Intertwined Mean-Field Approximation (NIMFA) [2], the infection probability v_i of node i that approximates the exact $E[X_i]$ is given by the following first-order nonlinear ordinary differential equation:

$$\frac{dv_i(t)}{dt} = \beta\sum_{j=1}^{N} a_{ij}v_j(t) - v_i(t)\big(\beta\sum_{j=1}^{N} a_{ij}v_j(t) + \delta\big). \quad (2)$$

A first-order mean-field approximation of the epidemic threshold $\tau_c^{(1)} = 1/\lambda_1(A)$, where $\lambda_1(A)$ is the spectral radius of the adjacency matrix A, was shown to be a lower bound, i.e., $\tau_c^{(1)} < \tau_c$, for the epidemic threshold [2] [17].

Heterogeneous infection is more realistic than the assumption of homogeneity in real-world spreading processes. For example, the transmission capacity per link in a data communication network can be different. In social networks, people who are keen on the social activities could spread a rumor more efficiently. The individual behavior leads to a difference in the infection rate β_i and the curing rate δ_i. The heterogeneous NIMFA model [12] [13] with the time-dependent infection rate $\beta_i(t)$ and the curing rate $\delta_i(t)$ of node i is described by

$$\frac{dv_i(t)}{dt} = (1-v_i(t))\sum_{j=1}^{N} a_{ij}\beta_j(t)v_j(t) - \delta_i(t)v_i(t) \quad (3)$$

In this paper, we focus on a method to adjusting the nodal infection rates $\beta_i(t)$ for the induced spreading. For simplicity and without lack of generality, we normalize the curing rate by $\delta_i(t)=1$ at any time for all nodes. Hence, the infection rate $\beta_i(t)$ equals the effective infection rate $\tau_i(t)$.

III. Static optimization for induced spreading

A. Problem statements

The SIS process can stay in the metastable state for a much longer time compared to the transient period if the effective infection rate τ is above the epidemic threshold τ_c. Induced spreading for a long term refers to the static optimization of the steady-state infection probability vector $\mathbf{v}_\infty = (v_{1\infty}, v_{2\infty}, \ldots, v_{N\infty})$ by adjusting the infection rates β_j for some nodes $j \in \mathcal{N}$. Static optimization is time-independent and has the advantage of operational simplicity. Specifically, the optimization problem aims to maximize the total steady-state infection probabilities of the nodes in the target set $\mathcal{S}$,

$$\max_{\mathbf{v}_\infty, \boldsymbol{\Delta\beta}} \quad J = \sum_{i\in S} v_{i\infty} \quad (4)$$

subject to the steady-state NIMFA equation with the infection rate $\beta_j = \hat{\beta} + \Delta\beta_j$ of node j,

$$(1-v_{i\infty})\sum_{j=1}^{N} a_{ij}(\hat{\beta}+\Delta\beta_j)v_{j\infty} - v_{i\infty} = 0, \quad i,j \in \mathcal{N} \quad (5)$$

where $\hat{\beta}$ is the original infection rate for all nodes, and the rate increment vector $\boldsymbol{\Delta\beta} = (\Delta\beta_1, \Delta\beta_2, \ldots, \Delta\beta_N)$ are the control variables. Also, we have the constraint on the total cost budget

$$\sum_{i=1}^{N} g(\Delta\beta_i) \le C, \quad i \in \mathcal{N} \quad (6)$$

where $g(\Delta\beta_i)$ is a convex function of the infection rate increment $\Delta\beta_i$, and C denotes a prescribed positive constant for the cost budget. Before solving this problem, we have Lemma 1 and Theorem 1 as follow:

Lemma 1: The steady-state infection probability $v_{i\infty}$ of any node i in the graph G_N monotonically increases with the infection rate β_j of any node j.

Proof: See Appendix 1.A. □

Theorem 1: The steady-state infection probability $v_{i\infty}$ of node i is not always concave with respect to the infection rate β_j for $i \neq j$.

Proof: See Appendix 1.B. □

Since the diagonal element $\frac{\partial^2 v_{i\infty}}{\partial \beta_i^2}$ in the Hessian matrix of the steady-state infection probability $\mathbf{v}_\infty$ with respect to the infection rate increment $\boldsymbol{\Delta\beta}$ could be positive according to Theorem 1, the Hessian matrix is not negative semi-definite. Thus, we conclude that the static optimization for induced SIS spreading is not a convex program, which cannot be solved by a simple method.

B. Global optimization by differential evolution

We further simplify the NIMFA constraint (5) by expressing $v_{i\infty}$ explicitly, and only dependent on the infection rates $\boldsymbol{\beta}$, but not on any other $v_{j\infty}$ for $j \neq i$. For any effective infection rate $\tau \geq 0$, the nonzero steady-state infection probability $v_{i\infty}$ of any node i in the NIMFA can expressed as a continued fraction [2] [15]. We define the k-level infection probability for node i as $v_{i\infty}^{(k)} = 1 - w_i(k)$, where the k-th convergent is $w_i(k) = \frac{1}{1+\sum_{j=1}^{N} a_{ij}\beta_j - \sum_{j=1}^{N} a_{ij}\beta_j w_j(k-1)}$ with starting value $w_i(0) = 0$ and $\lim_{k\to\infty} w_i(k) = 1 - v_{i\infty}$.

If the level k is large enough [2], the infection probability $v_{i\infty}^{(k)}$ is sufficiently close to $v_{i\infty}$. By approximating the infection probability $v_{i\infty}$ by $v_{i\infty}^{(k)}$, the optimization problem can be reduced to $\max_{\boldsymbol{\Delta\beta}} \sum_{i\in S} v_{i\infty}^{(k)}$ subject to the cost constraint (6). We further reduce the inequality constraint $\sum_{i=1}^{N} g(\Delta\beta_i) - C \leq 0$ to a penalty term by converting the objective to

$$\min_{\boldsymbol{\Delta\beta}} \quad -\sum_{i\in\mathcal{S}} v_i^{(k)} + \zeta \max\{0, \sum_{i=1}^{N} g(\Delta\beta_i) - C\} \tag{7}$$

where ζ is the penalty parameter. If the constraint is violated during the optimization process, the penalty term feeds the deviation to the objective function and draws the solution to the feasible region.

Since Problem (7) is multi-dimensional and nonlinear, we propose an approach based on the Differential Evolution (DE) algorithm to solve the constrained optimization problem. Differential evolution can approximate the global optima of a nonlinear program, which was proposed by Storn and Price [14]. The Differential Evolution algorithm resembles other traditional evolution algorithms like genetic algorithms (GA), and can represent the solution domain of $\boldsymbol{\Delta\beta}$ by real numbers. The Differential Evolution algorithm has the advantage of implementation simplicity over other non-genetic global optimization algorithms, e.g., the performance of simulated annealing algorithm is sensitive to the cooling rate and the initial solution. Also, the Differential Evolution algorithm [19] [20] is usually more efficient and accurate than several other optimization methods, e.g., simulated annealing and genetic algorithms. The proposed Differential Evolution method is based on population generation, mutation, crossover, and selection. The implementation is presented in Algorithm 1 (see Appendix 2).

IV. Dynamic Optimization for Induced Spreading

A. Problem statements

Dynamic optimization is a more general and more flexible method for the induced spreading. The infection rate increment $\boldsymbol{\Delta\beta}(t) = (\Delta\beta_1(t), \Delta\beta_2(t), \ldots, \Delta\beta_N(t))$ is time dependent in the dynamic optimization, which is different from the static optimization. Specifically, the dynamic optimization for the induced spreading aims to maximize the total cumulative infection probability $v_i(t)$ of the nodes in the target set $i \in \mathcal{S}$ in the time interval $[t_0, t_f]$, i.e.,

$$\max_{\boldsymbol{\Delta\beta}(t)} \quad J = \int_{t_0}^{t_f} \sum_{i\in\mathcal{S}} v_i(t)dt \tag{8}$$

subject to the NIMFA equation

$$\frac{dv_i(t)}{dt} = (1 - v_i(t)) \sum_{j=1}^{N} a_{ij}(\hat{\beta} + \Delta\beta_j(t))v_j(t) - v_i(t), \quad i, j \in \mathcal{N} \tag{9}$$

and the constraint on the cumulative cost in the time interval $[t_0, t_f]$

$$\int_{t_0}^{t_f} \sum_{i\in\mathcal{N}} g(\Delta\beta_i(t))dt \leq C, \quad i \in \mathcal{N} \tag{10}$$

where C is a prescribed cost budget. The dynamic optimization for induced SIS spreading is a control-affine nonlinear model [21] with the integral constraint (10), which cannot be solved by the standard methods for Linear Quadratic Regulator (LQR) problems.

B. The optimal solution

We first introduce an additional control variable z and rewrite the cost constraint (10) as

$$\frac{dz(t)}{dt} = \sum_{i\in\mathcal{N}} g(\Delta\beta_i(t)) \tag{11}$$

with $z(t_0) = 0$ and $z(t_f) = C$, where t_0 is the initial time and t_f is the final time. Then, the corresponding Hamiltonian is

$$H(\mathbf{v}, \boldsymbol{\Delta\beta}, \boldsymbol{\theta}, \mu) = \sum_{m\in\mathcal{S}} v_m + \mu \sum_{i\in\mathcal{N}} g(\Delta\beta_i(t)) \tag{12}$$

$$+ \sum_{i=1}^{N} \theta_i \left[(1 - v_i) \sum_{j=1}^{N} a_{ij}(\hat{\beta}_j + \Delta\beta_j)v_j - \delta v_i \right] \tag{13}$$

where the parameter $\boldsymbol{\theta} = (\theta_1, \theta_2, \ldots, \theta_N)$ and μ are undetermined. Next, we present the optimality conditions for the dynamic optimization.

Therorem 2: Suppose $\boldsymbol{\Delta\beta}^*(t)$ is an optimal control for the problem, and $\mathbf{v}^*(t)$ is the optimal solution with $\boldsymbol{\Delta\beta}(t) = \boldsymbol{\Delta\beta}^*(t)$. Then, there exist functions $\boldsymbol{\theta}^*(t)$ and $\mu^*(t)$, such that

$$\begin{cases} \dfrac{d\theta_i^*}{dt} = \chi_i + \theta_i^*(\sum_{j=1}^{N} a_{ij}\hat{\beta}_j v_j^* + 1) - \hat{\beta}_i \sum_{j=1}^{N} a_{ij}(1 - v_j^*)\theta_j^*, \\ \qquad\qquad\qquad\qquad\qquad\qquad\qquad\qquad i \in \mathcal{N} \\ \dfrac{d\mu^*}{dt} = 0 \end{cases} \tag{14}$$

with the terminal (transversality) conditions $\mu^*(t_f) = 0$ and $\theta_i^*(t_f) = 0$ for $i = 1, 2, \ldots, N$, where $\chi_i = -1$ for $i \in \mathcal{S}$, and $\chi_i = 0$ for $i \notin \mathcal{S}$.

Furthermore, the optimal control variable $\boldsymbol{\Delta\beta}^*(t)$ obeys

$$\frac{dg(\Delta\beta_i^*)}{d\Delta\beta_i^*} = -\frac{1}{\mu} v_i^* \sum_{j=1}^{N} a_{ij}(1 - v_j^*)\theta_j^*, \quad i \in \mathcal{N} \tag{15}$$

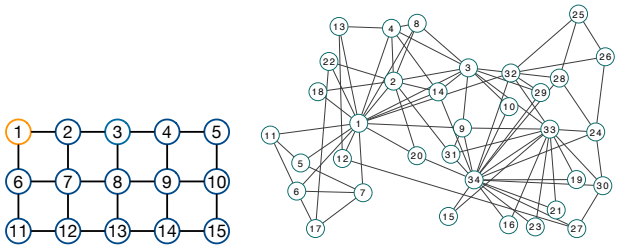

(a) (b)

Fig. 1: Illustration of the network topologies. (a) The lattice network $L_{3\times5}$ with $N = 15$ nodes. (b) The Karate network with $N = 34$ nodes.

Proof: According to the Pontryagin Maximum Principle [22], we can obtain the costate equations as

$$\begin{cases} \dfrac{d\theta_i^*}{dt} = -\dfrac{\partial H(\mathbf{v}^*, \boldsymbol{\Delta\beta}^*, \boldsymbol{\theta}^*, \mu^*)}{\partial v_i} \\ \dfrac{d\mu^*}{dt} = -\dfrac{\partial H(\mathbf{v}^*, \boldsymbol{\Delta\beta}^*, \boldsymbol{\theta}^*, \mu^*)}{\partial z} \end{cases} \tag{16}$$

for $t_0 \le t \le t_f$ and $i = 1, 2, \ldots, N$. Direct computing (16) yields to the equations (14). According to the optimality condition $H(\mathbf{v}^*, \boldsymbol{\Delta\beta}^*, \boldsymbol{\theta}^*, \mu^*) = \min_{\boldsymbol{\Delta\beta}_i} H(\mathbf{v}^*, \boldsymbol{\Delta\beta}, \boldsymbol{\theta}^*, \mu^*)$, we obtain that the optimal control $\Delta\beta_i^*(t)$ for $t_0 \le t \le t_f$ and $i = 1, 2, \ldots, N$ obeys

$$\frac{\partial H(\mathbf{v}^*, \boldsymbol{\Delta\beta}, \boldsymbol{\theta}^*, \mu^*)}{\partial u_i} = \mu^* \frac{dg(\Delta\beta_i^*)}{d\Delta\beta_i^*} + v_i^* \sum_{j=1}^{N} a_{ij}(1 - v_j^*)\theta_j^* = 0 \tag{17}$$

The optimality conditions include the state equations (9), the costate equations (14), and the stationary equations (15). □

The method of Adapted Forward Backward Sweep [21] with a Runge-Kutta fourth order scheme is applied to solve the optimality system. The convergence of this method is given in [23].

V. Numerical Results and Discussion

In this section, we investigate the behaviors of the induced SIS spreading by numerical results in some artificial and real networks. We define the quadratic cost function as $g(\Delta\beta_i) = (\Delta\beta_i)^2$ in the static method and $g(\Delta\beta_i(t)) = (\Delta\beta_i(t))^2$ in the dynamic method for $i = 1, 2, \ldots, N$. Since the control inputs are generally related to the external force or the electric current, the cumulative quadratic cost can be interpreted as the control energy [24] [25]. Applying the quadratic cost function also helps to compare the behavior of the induced spreading model with other existent models, e.g., LQR model. In order to guarantee the induced SIS spreading without extinction, we set the original constant infection rate $\hat{\beta} = \tau_c^{(1)} = \frac{1}{\lambda_1}$, and the infection probability $v_i(t) \approx 0$ for all nodes. Thus, the additional cost C for the induced spreading leads to a positive payoff on the infection probabilities of nodes.

A. Numerical results in the static optimization

1) Payoff versus cost budget for a single target node: We first investigate the impact of the cost budget C for targeting a single node in the static model. Fig. 2 presents the payoff $B = J(\boldsymbol{\Delta\beta}^*)$ as a function of the cost budget C for a single target node in the lattice network $L_{3\times5}$ in Fig. 1a. Fig. 2 shows that the payoff B of the target node for the same cost budget C depends on the topological properties of the target node. The target node with a larger degree (e.g., node 2 and 3) can obtain a higher payoff for the same cost budget C.

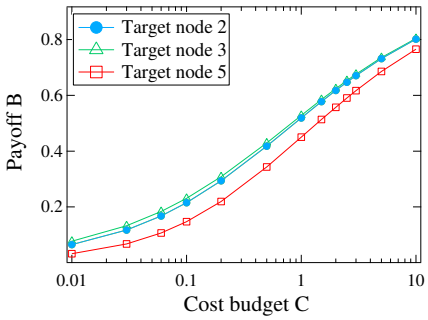

Fig. 2: The payoff $B = J(\boldsymbol{\Delta\beta}^*)$ in the static optimization as a function of the cost budget C for a single target node in the lattice network L_{3*5}.

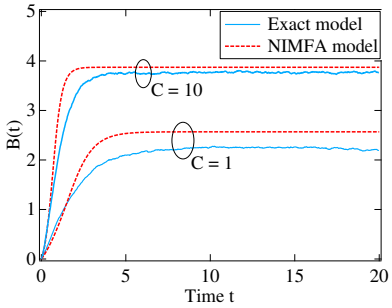

Fig. 3: The time-dependent payoff $B(t)$ after the static optimization with a determined cost budget C for $|\mathcal{S}| = 5$ randomly selected target nodes in the Karate network. The spreading processes start from the initial spreader 34. The payoff $B(t)$ in the exact model is obtained from the simulations based on Gillespie algorithm [18] by averaging 10^4 realizations.

2) Cost allocation in static optimization: We apply our methods to the Karate network [26] with $N = 34$ nodes, as illustrated in Fig. 1b. Figure 3 compares the time-dependent payoff $B(t)$ after the optimal cost allocation in the exact Markovian model and NIMFA. The payoffs $B(t)$ in both models follow a similar behavior, and the gap in the payoff between NIMFA and the exact model decreases for a larger cost budget C. Since NIMFA usually provides an upper bound of infection probability in the SIS spreading process [2], the exact payoff is also upper-bounded by the payoff in NIMFA.

For the static optimization, it is of practical significance to investigate the cost allocation on the nodes in the network. We define the average target distance $\bar{h}_i$ as the mean of all the minimum hops h_{ij} from node i to the target nodes $j \in \mathcal{S}$, i.e. $\bar{h}_i = \frac{1}{|\mathcal{S}|}\sum_{j\in\mathcal{S}} h_{ij}$, where $|\mathcal{S}|$ denotes the number of targets. Since the infection rate β_j does not directly influence the infection probability $v_{j\infty}$ of node j, the actual minimum hops of the influence on infection probability $v_{j\infty}$ by the infection rate β_j is 2 hops. Hence, we set $h_{jj} = 2$ instead of $h_{jj} = 0$ to compute the average target distance $\bar{h}_j$ for the target node $j \in \mathcal{S}$.

Fig. 4 shows the relation between the optimal rate increment

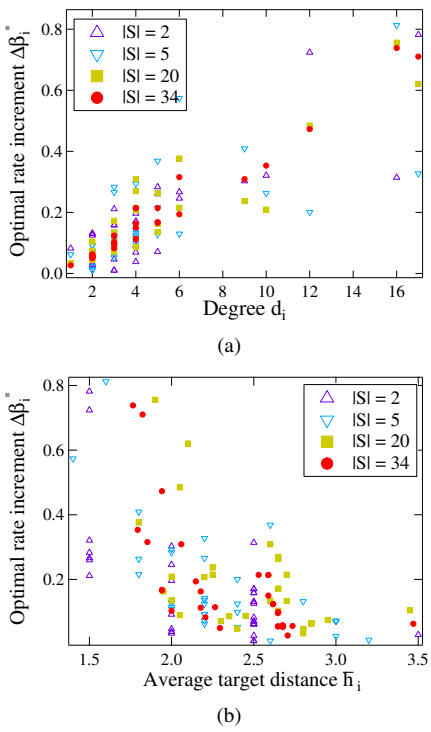

Fig. 4: (a) The relation between the optimal rate increment $\Delta\beta_i^*$ on node i and the degree d_i for different number of target nodes $|\mathcal{S}|$. (b) The relation between the optimal rate increment $\Delta\beta_i^*$ on node i and the average target distance $\bar{h}_i$. The target nodes are randomly selected in the Karate network with $N = 34$ nodes.

$\Delta\beta_i^*$ and the topological properties of node i, e.g., the degree d_i and the average distance $\bar{h}_i$, for different fraction of targets $|\mathcal{S}|$. We illustrate that both the degree d_i and the average distance $\bar{h}_i$ are highly related to the cost allocation on nodes. Specifically, the node with a relatively high degree d_i and a shorter average distance $\bar{h}_i$ to the target nodes usually has a larger infection rate increment $\Delta\beta_i^*$. The steady-state infection probability [2] approximates

$$v_{i\infty} \approx 1 - \frac{1}{1 + \sum_{j=1}^{N} a_{ij}\beta_j \left(1 - \frac{1}{1+\sum_{k=1}^{N} a_{jk}\beta_k}\right)} \approx 1 - \frac{1}{1 + \sum_{j=1}^{N} a_{ij}\beta_j \left(1 - \frac{1}{1+d_j\beta_k}\right)} \quad (18)$$

assuming that the infection rate β_k of the neighbors of node j are the same. The infection rate increment on the node with a larger degree d_j among the neighbors of node i could provide a larger payoff on the infection probability $v_{i\infty}$ of the target node i. If the fraction of target nodes $\frac{|\mathcal{S}|}{N}$ is relatively large, the cost allocated on the node with a larger degree can benefit more neighbors of this node, which leads to a stronger correlation between the infection rate increment $\Delta\beta_i^*$ and the degree d_i. In Appendix 3, we show more numerical results about the relation between the optimal rate increment $\Delta\beta_i^*$ and the degree d_i.

B. Numerical results in the dynamic optimization

1) Induced strategy for a single target node: Dynamic optimization is concerned with the spreading trajectory for steering the viruses from the initial spreader to the target nodes. We first investigate the behavior of the optimal induced spreading for a single target node. Fig. 5 shows the optimal control $\boldsymbol{\Delta\beta^*}(t)$ in the lattice network $L_{3\times5}$ in Fig. 1a with the single target node 4 and the initial spreader 1, which illustrates that the behavior of the optimal rate increment $\boldsymbol{\Delta\beta}^*(t)$ depends on the cost budget C. For a small cost C (e.g., $C = 0.5$ in Fig. 5(a)), most of the cost budget is allocated to the nodes on the shortest paths from the initial spreader to the target node. For a large cost C (e.g., $C = 10$ in Fig. 5(b)), the time-dependent optimal control $\boldsymbol{\Delta\beta^*}(t)$ can be divided into two periods: first steering the viruses from the initial spreader to the target node, and then the control inputs on the neighbors (e.g. $\Delta\beta_5^*(t), \Delta\beta_8^*(t), \Delta\beta_9^*(t)$) of the target node 1 stay in a meta-steady state (e.g., $t = 1.5 - 4$) to maintain the infection probability of the target node.

We define the payoff $B = J(\boldsymbol{\Delta\beta}^*(t))$ with the optimal control $\boldsymbol{\Delta\beta}^*(t)$ for the SIS induced spreading. Fig. 6 shows the payoff B as a function of the cost budget C for a single target node in the lattice network $L_{3\times5}$. The logarithmic payoff $\log B$ increase faster than a linear function with the logarithmic cost budget $\log C$ for small cost budgets C, while the sub-figure in Fig. 6 shows the relation $B \sim \log C$ for larger cost budgets C. This result is in agreement with the above discussion on the behavior of the optimal control $\boldsymbol{\Delta\beta^*}(t)$. The small cost budget mainly contributes to steering the viruses from the initial spreader to the target nodes, and the payoff increases relatively faster. The larger cost budget is mainly allocated to the neighbors of the target nodes, and the payoff presents diminishing returns, which approximates the induced strategy in the static optimization (e.g., Fig. 2).

2) Cost scaling with the topological properties of a single target node: Further, we investigate the cost scaling with the topological properties of a single target node. Fig. 7 shows the minimum cost C_{ij}^* that makes the target node v_j be infected at least once in the time interval $[0, 5]$, i.e., the cumulative infection probability $J = \int_0^5 v_j(t)dt \geq 1$, in the lattice $L_{3\times5}$ with the initial infection node i. Intuitively, the minimum cost C_{ij}^* depends on the shortest distance (minimum hops) h_{ij} from the initial spreader i to the target j because all the nodes on the paths should be allocated some cost to steer the viruses to the target. Meanwhile, Fig. 7a illustrates that the minimum cost C_{ij}^* is also coupled to the number of paths from the initial spreader i to the target node j, i.e., a larger number of paths leads to a less cost C_{ij}^*.

Inspired by Thompson's principle [27] that the minimum energy dissipation is related to the effective resistance in electric circuits, we introduce the effective resistance ω_{ij} between node i and node j as $\omega_{ij} = (Q_{ii}^\dagger + Q_{jj}^\dagger - 2(Q_{ij}^\dagger))$, where $Q^\dagger$ is the pseudoinverse of the Laplacian matrix Q of the network topology. Van Mieghem *et al.* [28] shows that the best conducting node j in a graph as the minimizer of the diagonal element $Q_{jj}^\dagger$ of the pseudoinverse matrix $Q^\dagger$. Fig. 7b shows that the relation between the optimal cost C_{1j}^* with the initial spreader 1 and the normalized shortest distance $\frac{h_{1j}}{\max_{j\in N} h_{1j}}$ as well as the normalized effective resistance $\frac{\omega_{1j}}{\max_{j\in N} \omega_{1j}}$. We obtain that the Pearson correlation coefficient ρ_h between the minimum cost C_{1j}^* and the hops h_{1j} is equal to $\rho_h =$

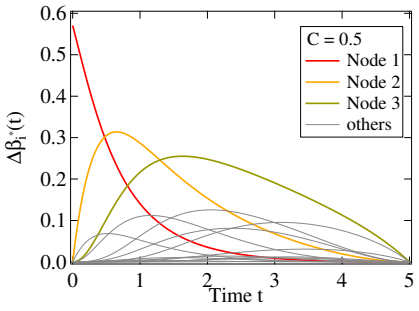

(a) C = 10

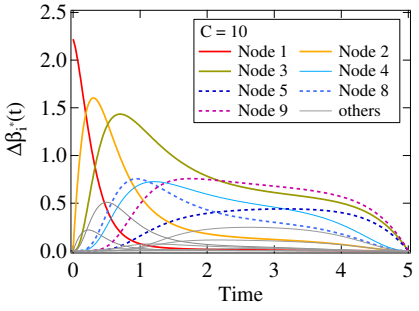

(b) C = 0.5

Fig. 5: The optimal control $\boldsymbol{\Delta\beta^*}(t)$ for the target node 4 with the initial spreader 1 in the lattice network L_{3*5}. The initial time is $t_0 = 0$ and the final time is $t_f = 5$. (a) The optimal control $\boldsymbol{\Delta\beta^*}(t)$ for the cost budget $C = 0.5$; (b) The optimal control $\boldsymbol{\Delta\beta^*}(t)$ for the cost budget $C = 10$.

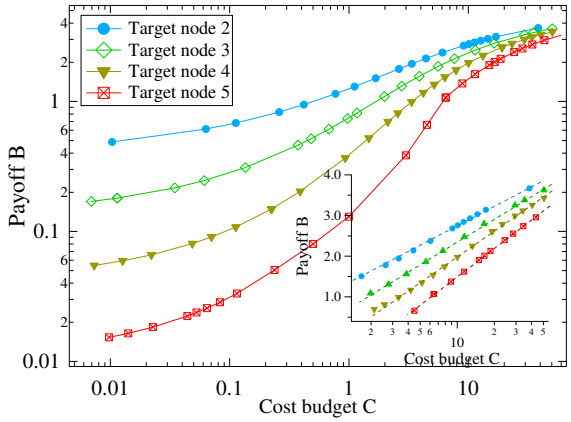

Fig. 6: The payoff $B = J(\boldsymbol{\Delta\beta}^*(t))$ as a function of the cost C with the initial spreader 1 for a single target node in the lattice network L_{3*5}.

0.907. For the Pearson correlation coefficient ρ_ω between the minimum cost C^*_{1j} and the effective resistance ω_{1j}, we obtain $\rho_\omega = 0.983$. This demonstrates that the effective resistance is a good metric for the cost scaling for a single target node in the induced spreading.

3) Cost scaling with the fraction of target nodes : In a linear system, the optimal control energy (cost) C^*_{max} for targeted controlling in the worst case [29] has the scaling equation $\log C^*_{max} \sim \frac{|\mathcal{S}|}{N}$, which implies that the cost C^*_{max} increases fast with the fraction $s = \frac{|\mathcal{S}|}{N}$ of target nodes. We will show that the behavior of energy scaling with the fraction of target nodes in the SIS process is different. We compute the optimal cost $C^*(s)$ subject to the constraint on the average infection

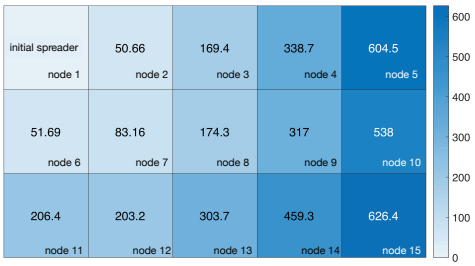

(a)

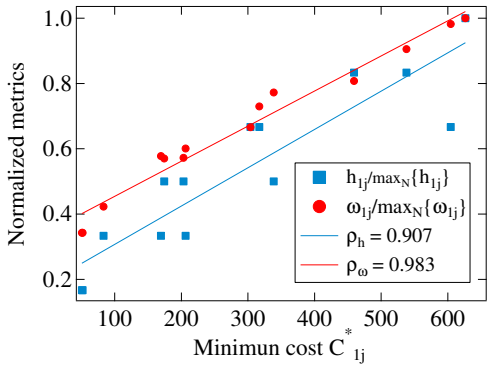

(b)

Fig. 7: (a) The minimum cost C^*_{1j} to make the target node v_j for $j = 2, 3, \ldots, 15$ be infected at least once in the time interval $[0, 5]$, i.e., $\int_0^5 v_j(t)dt \geq 1$, in the Lattice network $L_{3\times5}$. The spreading starts from the initial spreader 1; (b) The relation between the minimum cost C^*_{1j} and the normalized shortest distance $\frac{h_{1j}}{\max_{j\in N} h_{1j}}$ as well as the normalized effective resistance $\frac{\omega_{1j}}{\max_{j\in N} r_{1j}}$.

frequency $\frac{1}{|\mathcal{S}|}\int_{t_0}^{t_f}\sum_{i\in\mathcal{S}} v_i(t)dt \geq 1$ of $|\mathcal{S}|$ target nodes in the SIS spreading process. Then, we can obtain the average optimal cost $E[C^*(s)]$ with randomly selected $|\mathcal{S}|$ target nodes in the network for multiple realizations.

In a star network $K_{1,N}$ with an initial central spreader, the infection rate increment $\Delta\beta^*_1(t)$ on the central node for a leaf target could steer the viruses to other leaves simultaneously. Thus, the increasing fraction $s = \frac{|\mathcal{S}|}{N}$ of the target leaves influences little on the required average minimum cost $E[C^*(s)]$, as shown in Fig. 8a. Fig. 8b illustrates that the normalized average cost

$$\frac{E[C^*(s)]}{E[C^*(1/N)]} \sim \eta \log \frac{|\mathcal{S}|}{N} \tag{19}$$

in the Erdős-Rényi (ER) random network $G_p(N)$ with link density p, where η is a parameter. The cost scaling law (19) is different from targeting control in linear control systems [29]. In linear systems, the control input for controlling a target could introduce perturbances for another target, which leads to more additional effort to control multiple targets. In the spreading process, the cost allocated on one node always benefit multiple targets by steering the viruses to them. Further, Fig. 8b shows that the parameter η in (19) is coupled to the network topology and decreases with the increasing link density p in the ER random network. More nodes can benefit from the cost allocated on a single node in a denser network with a higher average degree. Thus, the less additional cost is

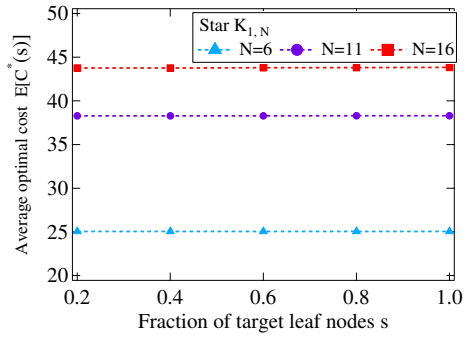

(a)

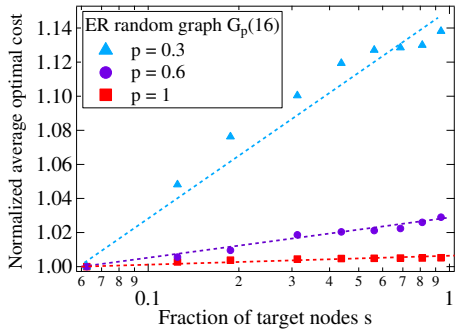

(b)

Fig. 8: (a) The optimal cost $C^*(s)$ as a function of the fraction of leaf targets in the star $K_{1,N}$ with N leaf nodes. We set the central node as the initial spreader and the leaf nodes as the targets. (b) The normalized average cost $\frac{E[C^*(s)]}{E[C^*(1/N)]}$ as a function of the fraction of target nodes $s = \frac{|\mathcal{S}|}{N}$ in the ER random network $G_p(16)$ with the link density p. Each average optimal cost $E[C^*(s)]$ is obtained by 20 realizations. The time interval of controlling is $[t_0, t_f]$ with $t_0 = 0$ and $t_f = 5$.

required to steer the virus to additional targets, which translates to a smaller η.

C. Comparison between the static optimization and the dynamic optimization

Two optimization methods, static and dynamic optimizations, are proposed for the induced SIS spreading in the network. We now compare their performance in the Karate network. We rewrite the constraint (6) in the static method as $\sum_{i=1}^{N} g(\Delta\beta_i) \leq \frac{C}{t_f - t_0}$ where C is also the cost budget in the dynamic method, and both methods have a same cost budget C in the time interval $[t_0, t_f]$. Then, we compute the payoff in the static method by $B = \int_{t_0}^{t_f} \sum_{i\in\mathcal{S}} v_i(t)$ by the NIMFA equation (2) with the constant optimal solution $\boldsymbol{\Delta\beta}^*(t) = \boldsymbol{\Delta\beta}^*$ for any time in the static optimization.

Fig. 9a shows that the dynamic method generally outperforms the static method for different cost budgets C. Specifically, the difference between both methods exhibits a maximum around $C = 10$, and then decays slowly with the cost budget C. Fig. 9b shows the optimal infection rate increment $\boldsymbol{\Delta\beta}^*(\boldsymbol{t})$ for the target node 25 with the initial spreader 2, where the optimal control $\boldsymbol{\Delta\beta}^*$ is time-dependent for the dynamic optimization and constant for the static optimization. The optimal control vector $\boldsymbol{\Delta\beta}^*(\boldsymbol{t})$ for the dynamic optimization (solid line) exhibits a metastable state from $t = 1-4$, and the optimal control $\boldsymbol{\Delta\beta}^*$ for the static optimization (dash line) approximates the dynamic control $\boldsymbol{\Delta\beta}^*(\boldsymbol{t})$ in the metastable state. Moreover, Fig. 9c shows the normalized cost allocated on the node i.e., $\frac{t_f - t_0}{C} g(\Delta\beta_i^*)$ for the static optimization and $\frac{1}{C}\int_{t_0}^{t_f} g(\Delta\beta_i^*(t))$ for the dynamic, versus the cost budget C. The difference between the normalized cost in both optimizations also becomes smaller for a larger cost budget C, which demonstrates that the dynamic induced strategy approaches the static strategy with increasing cost budget C. Thus, we suggest to apply the dynamic optimization for a limited cost budget while the performance of the static optimization is already good enough for an adequate cost budget.

VI. Related Work

Virus spread in networks has been deeply studied in recent years [1]. The previous works on the Susceptible-Infected-Susceptible (SIS) model involve the epidemic threshold [12] [16] [17], the average fraction of infection nodes over time [30] and time-dependent properties in SIS processes [18] [31]. The N-intertwined mean-field approximation [2] is a reasonably accurate approximation of the exact SIS epidemics on a network [32].

Some previous research has investigated epidemics control [4], which aims to stop the spreading as soon as possible. The static optimization of epidemics control can be converted to a spectral control problem, where a fixed number of resources must be optimally allocated to best mitigate the effects of a disease. Preciado *et al.* [6] propose the budget-constrained allocation problem and present a solution framework based on Geometric Programming. Some greedy strategies of link removal based on the topological properties of links for spectral control are proposed [5] [33]. However, the solution by the greedy strategies may deviate much from the optimum in some worst cases [34]. The dynamic optimization, i.e., the optimal control, of a deterministic epidemic is proposed in [35] [36] and solved by using Pontryagin's maximum principle. The epidemic processes on a network allow each individual to have its own state, which makes the control strategy depend on the network topology [37] [38].

The problem of influence maximization [39] has a similar goal with the optimal induced spreading but different control variables. Influence maximization aims to find the optimal initial state (initial spreader) of a spreading, while the optimal induce spreading aims to adjust the parameters of the SIS model under the assumption that the initial spreaders are fixed.

VII. Conclusion

In this paper, we explore the induced SIS spreading on networks, which aims to steer the viruses to the target nodes as much as possible by adjusting the nodal infection rates under a limited cost budget. We provide two frameworks for the optimal induced spreading: the static optimization and the dynamic optimization. We propose the algorithms for both the optimization problems and further investigate the behavior of the induced strategy by numerical results on networks with the constraint of a quadratic cost function.

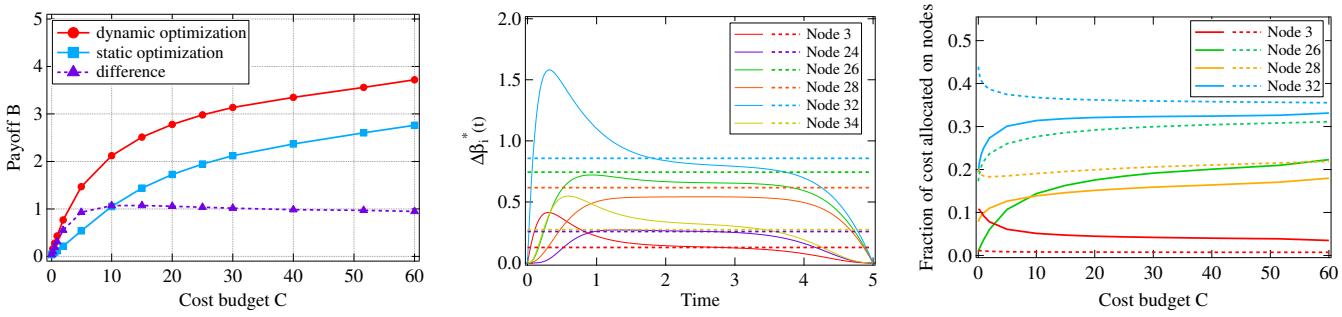

Fig. 9: (a) The comparison of the payoff B in the static optimization and the dynamic optimization with the cost budget C in the Karate network. The initial spreader is node 2 and the target node is node 25. The time interval of controlling is $[0, 5]$. (b) The optimal control $\boldsymbol{\Delta\beta^*}$ in the static method (dash lines) and $\boldsymbol{\Delta\beta^*(t)}$ in the dynamic method (solid lines) with the cost budget $C = 10$ in the Karate network. (c) The normalized cost allocated on the node i.e., $\frac{t_f - t_0}{C} g(\Delta\beta_i^*)$ for the static optimization and $\frac{1}{C}\int_{t_0}^{t_f} g(\Delta\beta_i^*(t))$ as a function of the cost budget C.

In the static optimization, the optimal infection rate increment of each node is highly related to the degree and its average hops to the targets, while the degree dominates the nodal infection rate increment for a large fraction of targets. In the dynamic optimization, we show that the time-dependent optimal infection rate increment exhibits two periods for a large cost budget: steering the viruses from the initial spreader to the target, and maintaining the infection probability of the target by its neighbors. For a single target node, we show that the effective resistance could be a good metric to indicate the cost scaling. Further, we illustrate that the cost scaling with the fraction of targets has different behaviors to that of the targeted controlling in linear systems, because the cost for increasing the infection rate of one node usually benefits the infection probabilities of multiple targets. Finally, we show that the dynamic induced strategy approximates the static for a large cost budget.

Some problems of practical significance merit further study. First, the induced SIS spreading problem can be generalized to guide the infection to some target nodes while avoiding some other specific nodes as much as possible. We suspect that some results presented in this paper, such as the cost scaling with the fraction of the targets, could change for the generalized problem. Second, the topological properties of the most efficient spreader [40] with a minimum total cost for the induced spreading is worthy of study.

APPENDIX I
PROOFS OF LEMMA AND THEOREM

A. Proof for Lemma 1

Proof: According to the NIMFA equation (2), we have the steady-state equation

$$\left(\text{diag}(1 - v_{i\infty})A\text{diag}(\beta_j) - I\right)\mathbf{v}_\infty = 0 \qquad (20)$$

By differentiation with respect to β_j, we obtain

$$\begin{cases} \sum_{k=1}^{N} a_{ik}\beta_k \frac{\partial v_k}{\partial \beta_i} - \frac{1}{(1-v_{i\infty})^2}\frac{\partial v_{i\infty}}{\partial \beta_i} = 0 & \text{if } i = j \\ \sum_{k=1}^{N} a_{jk}\beta_k \frac{\partial v_k}{\partial \beta_i} - \frac{1}{(1-v_{j\infty})^2}\frac{\partial v_{j\infty}}{\partial \beta_i} + a_{ji}v_{i\infty} = 0 & \text{if } i \neq j \end{cases}$$

Written in matrix form, we have

$$\left(A\text{diag}(\beta_i) - \text{diag}\left((1-v_{i\infty})^{-2}\right)\right)T_1 + A\text{diag}(\mathbf{v}_\infty) = 0 \quad (21)$$

where the element of the matrix T_1 in the k-th row and the q-th column is $T_{1(kq)} = \frac{\partial v_{k\infty}}{\partial \beta_q}$. For the matrix $M_1 := A\text{diag}(\beta_i) - \text{diag}\left((1-v_{i\infty})^{-2}\right)$, it has been proved that all entries in M_1^{-1} are non-positive [12], which implies that all entries in $T_1 = M_1^{-1}(-A\text{diag}(\mathbf{v}_\infty))$ are non-negative. □

B. Proof for Theorem 1

Proof: By differentiation of (21) with respect to β_j, we obtain

$$\begin{cases} \sum_{k=1}^{N} a_{ik}\beta_k \frac{\partial^2 v_k}{\partial {\beta_i}^2} - \frac{1}{(1-v_{i\infty})^2}\frac{\partial^2 v_{i\infty}}{\partial {\beta_i}^2} \\ \qquad - \frac{2}{(1-v_{i\infty})^3}\left(\frac{\partial v_{i\infty}}{\partial \beta_i}\right)^2 = 0 & \text{if } i = j \\ \sum_{k=1}^{N} a_{jk}\beta_k \frac{\partial^2 v_k}{\partial {\beta_i}^2} - \frac{1}{(1-v_{j\infty})^2}\frac{\partial^2 v_{j\infty}}{\partial {\beta_i}^2} \\ -\frac{2}{(1-v_{j\infty})^3}\left(\frac{\partial v_{j\infty}}{\partial \beta_i}\right)^2 + 2a_{ji}\frac{\partial v_{i\infty}}{\partial \beta_i} = 0 & \text{if } i \neq j \end{cases}$$

Written in matrix form, we have

$$\left(A\text{diag}(\beta_i) - \text{diag}\frac{1}{(1-v_{i\infty})^2}\right)T_2 + 2A\text{diag}\left(\frac{\partial v_{i\infty}}{\partial \beta_i}\right) - 2\text{diag}\left((1-v_{i\infty})^{-3}\right)T_1^{(2)} = 0 \quad (22)$$

where the element of the matrix T_2 in the k-th row and the q-th column is $T_{2(kq)} = \frac{\partial^2 v_{k\infty}}{\partial {\beta_q}^2}$, and $T_{1(kq)}^{(2)} = \left(\frac{\partial v_{k\infty}}{\partial \beta_q}\right)^2$ for the matrix $T_1^{(2)}$. In the matrix $M_2 := 2A\text{diag}\left(\frac{\partial v_{i\infty}}{\partial \beta_i}\right) -$

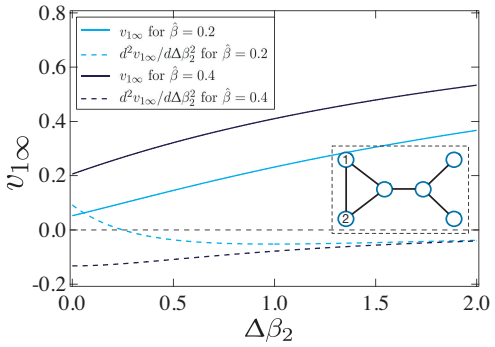

Fig. 10: The infection probability $v_{1\infty}^{(3)}$ and its second order partial derivative $\partial^2 v_{1\infty}^{(3)}/\partial\Delta\beta_2^2$ as the function of $\Delta\beta_2$ with different original infection rate $\hat{\beta}$ in the example network G_6.

$2\text{diag}\left((1-v_{i\infty})^{(-3)}\right) T_1^{(2)}$, the entries follows

$$M_{2(ij)} = 2\frac{\partial v_{i\infty}}{\partial\beta_j}\left(a_{ij} - (1-v_{i\infty})^{-3}\frac{\partial v_{i\infty}}{\partial\beta_j}\right). \tag{23}$$

Invoking that $\frac{\partial v_{i\infty}}{\partial\beta_i}$ is always non-negative, the entries $M_{2(ij)}$ in M_2 could be non-positive only when $a_{ij} = 0$. Unfortunately, the sign of $\frac{\partial^2 v_{i\infty}}{\partial\beta_j{}^2}$ cannot be determined and could be positive. Therefore, the infection probability $v_{i\infty}$ is not always concave to β_j. We present a counterexample in Fig. 10. □

APPENDIX II
DIFFERENTIAL EVOLUTION ALGORITHM

We propose the Differential Evolution algorithm to solve the static induced SIS spreading problem. The implementation is as follow.

Population generation: The jth vector of the population at the kth generation is denoted as $\boldsymbol{\Delta\beta}_j(k) = \{\Delta\beta_{1,j}(k), \Delta\beta_{2,j}(k), \ldots, \Delta\beta_{N,j}(k)\}$. The initial population vectors are generated considering the constraints on the variables. We choose the initial generation as $\Delta\beta_{i,j}(1) = \kappa\Delta\overline{\beta}_i$, where κ is a uniformly distributed random number on interval $[0, 1]$.

Mutation: Mutation is a change or perturbation with a random element. We choose three different vectors with indices $r_1, r_2, r_3 \in \{1, 2, \ldots, N_p\}$ and construct the mutated vector $\boldsymbol{\Delta\beta}_j(k+1)$ at the $(k+1)$th generation as $\boldsymbol{\Delta\beta}_j(k+1) = \boldsymbol{\Delta\beta}_{r_1}(k) + F(\boldsymbol{\Delta\beta}_{r_2}(k) - \boldsymbol{\beta}_{r_3}(k))$, where F is a uniformly distributed random number on interval $[F_{min}, F_{max}]$.

Crossover: Crossover is to enhance the potential diversity of the population, which obeys

$$\Delta\beta_{i,j}(k+1) = \begin{cases} \Delta\beta_{i,j}(k+1) & \text{if } \kappa \le R \\ \Delta\beta_{i,j}(k) & \text{otherwise} \end{cases}$$

where R is the crossover rate, which is a prescribe parameter of the algorithm.

Selection: DE uses the greedy strategy to choose the better vector to be the population in the next generation. The selection operation is described as

$$\boldsymbol{\Delta\beta}_j(k+1) = \begin{cases} \boldsymbol{\Delta\beta}_j(k+1) & \text{if } J(\boldsymbol{\Delta\beta}_j(k+1)) \le J(\boldsymbol{\Delta\beta}_j(k)) \\ \boldsymbol{\Delta\beta}_j(k) & \text{otherwise} \end{cases}$$

The process of the Differential Evolution algorithm for the static induced spreading problem is presented in Algorithm 1.

Algorithm 1 Differential Evolution algorithm

Inputs:
  A, β, M, K, ϵ
Initialization:
  Set $k \leftarrow 1$
  Generate initial populations
  $\boldsymbol{\Delta\beta}_j(1), j \in \{1, 2, \ldots, N_P\}$
for $k = 1$ to K **do**
  for $j = 1$ to N_P **do**
    Select randomly $r_1 \neq r_2 \neq r_3$ with $r_1, r_2, r_3 \in \{1, 2, \ldots, N_P\} : j_{rand} = randint(1, N)$
    for $i = 1$ to N **do**
      if $rand_j(0, 1) < R$ or $j = j_{rand}$ **then**
        $\Delta\beta_{i,j}(k+1) = \Delta\beta_{i,r_1}(k) + F(\Delta\beta_{i,r_2}(k) - \Delta\beta_{i,r_3}(k))$
      else
        $\Delta\beta_{i,j}(k+1) = \Delta\beta_{i,j}(k)$
      end if
    end for
    if $J(\boldsymbol{\Delta\beta}_j(k+1)) \le J(\boldsymbol{\Delta\beta}_j(k))$ **then**
      $\boldsymbol{\Delta\beta}_j(k+1) \leftarrow \boldsymbol{\Delta\beta}_j(k+1)$
    else
      $\boldsymbol{\Delta\beta}_j(k+1) \leftarrow \boldsymbol{\Delta\beta}_j(k)$
    end if
  end for
  $k \leftarrow k + 1$
end for

APPENDIX III
MORE NUMERICAL RESULTS

Figure 11 shows the relation between the optimal rate increment $\Delta\beta_i^*$ on node i and the degree d_i in Les Misérables network [41] and the dolphins network [42]. Figure 11 shows that the correlation between the optimal rate increment $\Delta\beta_i^*$ and the degree d_i usually becomes stronger with the increasing number of target nodes $|\mathcal{S}|$.

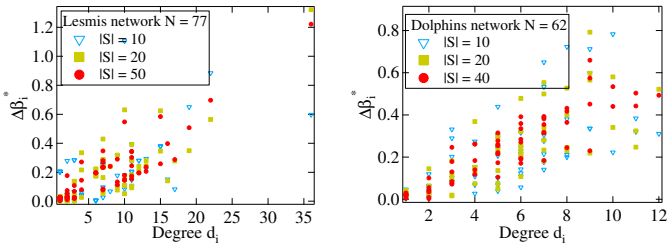

(a) Les Misérables network (b) Dolphins network

Fig. 11: The relation between the optimal rate increment $\Delta\beta_i^*$ on node i and the degree d_i for different number of target nodes $|\mathcal{S}|$. The target nodes are randomly selected.

REFERENCES

[1] R. Pastor Satorras, C. Castellano, P. Van Mieghem, and A. Vespignani, "Epidemic processes in complex networks," *Reviews of modern physics*, vol. 87, no. 3, p. 925, 2015.
[2] P. Van Mieghem, J. Omic, and R. Kooij, "Virus spread in networks," *IEEE/ACM Transactions on Networking*, vol. 17, no. 1, pp. 1–14, 2009.

[3] S. Roy, M. Xue, and S. K. Das, "Security and discoverability of spread dynamics in cyber-physical networks," *IEEE Transactions on Parallel and Distributed Systems*, vol. 23, no. 9, pp. 1694–1707, 2012.

[4] C. Nowzari, V. M. Preciado, and G. J. Pappas, "Analysis and control of epidemics: a survey of spreading processes on complex networks," *IEEE Control Systems*, vol. 36, no. 1, pp. 26–46, 2016.

[5] P. Van Mieghem, D. Stevanović, F. Kuipers, C. Li, R. van De Bovenkamp, D. Liu, and H. Wang, "Decreasing the spectral radius of a graph by link removals," *Physical Review E*, vol. 84, no. 1, p. 016101, 2011.

[6] V. M. Preciado, M. Zargham, C. Enyioha, A. Jadbabaie, and G. J. Pappas, "Optimal resource allocation for network protection against spreading processes," *IEEE Transactions on Control of Network Systems*, vol. 1, no. 1, pp. 99–108, 2014.

[7] Y. Sun, L. Ma, A. Zeng, and W.-X. Wang, "Spreading to localized targets in complex networks," *Scientific reports*, vol. 6, p. 38865, 2016.

[8] P. J. Roberts and C. J. Der, "Targeting the Raf-MEK-ERK mitogen-activated protein kinase cascade for the treatment of cancer," *Oncogene*, vol. 26, no. 22, p. 3291, 2007.

[9] W. Lu, S. Xu, and X. Yi, "Optimizing active cyber defense," in *International Conference on Decision and Game Theory for Security*. Springer, 2013, pp. 206–225.

[10] A. Y. Lokhov and D. Saad, "Optimal deployment of resources for maximizing impact in spreading processes," *Proceedings of the National Academy of Sciences*, p. 201614694, 2017.

[11] B. Karrer and M. E. Newman, "Message passing approach for general epidemic models," *Physical Review E*, vol. 82, no. 1, p. 016101, 2010.

[12] P. Van Mieghem and J. Omic, "In-homogeneous virus spread in networks," *arXiv preprint arXiv:1306.2588*, 2013.

[13] B. Qu and H. Wang, "SIS epidemic spreading with heterogeneous infection rates," *IEEE Transactions on Network Science and Engineering*, vol. 4, no. 3, pp. 177–186, 2017.

[14] R. Storn and K. Price, "Differential evolution – a simple and efficient heuristic for global optimization over continuous spaces," *Journal of global optimization*, vol. 11, no. 4, pp. 341–359, 1997.

[15] P. Van Mieghem, *Performance analysis of complex networks and systems*. Cambridge University Press, 2014.

[16] C. Castellano and R. Pastor-Satorras, "Thresholds for epidemic spreading in networks," *Physical Review Letters*, vol. 105, no. 21, p. 218701, 2010.

[17] P. Van Mieghem and R. van de Bovenkamp, "Non-Markovian infection spread dramatically alters the susceptible-infected-susceptible epidemic threshold in networks," *Physical Review Letters*, vol. 110, no. 10, p. 108701, 2013.

[18] Z. He and P. Van Mieghem, "The spreading time in SIS epidemics on networks," *Physica A: Statistical Mechanics and its Applications*, vol. 494, pp. 317–330, 2018.

[19] K. Price, R. M. Storn, and J. A. Lampinen, *Differential evolution: a practical approach to global optimization*. Springer Science & Business Media, 2006.

[20] M. M. Ali and A. Törn, "Population set-based global optimization algorithms: some modifications and numerical studies," *Computers & Operations Research*, vol. 31, no. 10, pp. 1703–1725, 2004.

[21] S. Lenhart and J. T. Workman, *Optimal control applied to biological models*. Crc Press, 2007.

[22] D. Liberzon, *Calculus of variations and optimal control theory: a concise introduction*. Princeton University Press, 2011.

[23] M. McAsey, L. Mou, and W. Han, "Convergence of the forward-backward sweep method in optimal control," *Computational Optimization and Applications*, vol. 53, no. 1, pp. 207–226, 2012.

[24] F. L. Lewis, D. Vrabie, and V. L. Syrmos, *Optimal control*. John Wiley & Sons, 2012.

[25] J. A. Primbs, V. Nevistić, and J. C. Doyle, "Nonlinear optimal control: A control lyapunov function and receding horizon perspective," *Asian Journal of Control*, vol. 1, no. 1, pp. 14–24, 1999.

[26] W. W. Zachary, "An information flow model for conflict and fission in small groups," *Journal of anthropological research*, vol. 33, no. 4, pp. 452–473, 1977.

[27] P. G. Doyle and J. L. Snell, *Random walks and electric networks*. Mathematical Association of America, 1984, vol. 22.

[28] P. Van Mieghem, K. Devriendt, and H. Cetinay, "Pseudoinverse of the laplacian and best spreader node in a network," *Physical Review E*, vol. 96, no. 3, p. 032311, 2017.

[29] I. Klickstein, A. Shirin, and F. Sorrentino, "Energy scaling of targeted optimal control of complex networks," *Nature communications*, vol. 8, p. 15145, 2017.

[30] P. Van Mieghem, "Approximate formula and bounds for the time-varying susceptible-infected-susceptible prevalence in networks," *Physical Review E*, vol. 93, no. 5, p. 052312, 2016.

[31] A. Ganesh, L. Massoulié, and D. Towsley, "The effect of network topology on the spread of epidemics," in *INFOCOM 2005. 24th Annual Joint Conference of the IEEE Computer and Communications Societies. Proceedings IEEE*, vol. 2. IEEE, 2005, pp. 1455–1466.

[32] C. Li, R. van de Bovenkamp, and P. Van Mieghem, "The SIS mean-field N-intertwined and Pastor-Satorras & Vespignani approximation: a comparison," *Phys. Rev. E*, vol. 86, no. 2, p. 026116, 2012.

[33] A. N. Bishop and I. Shames, "Link operations for slowing the spread of disease in complex networks," *EPL (Europhysics Letters)*, vol. 95, no. 1, p. 18005, 2011.

[34] M. Zargham and V. Preciado, "Worst-case scenarios for greedy, centrality-based network protection strategies," in *Information Sciences and Systems (CISS), 2014 48th Annual Conference on*. IEEE, 2014, pp. 1–6.

[35] R. Morton and K. H. Wickwire, "On the optimal control of a deterministic epidemic," *Advances in Applied Probability*, vol. 6, no. 4, pp. 622–635, 1974.

[36] G. A. Forster and C. A. Gilligan, "Optimizing the control of disease infestations at the landscape scale," *Proceedings of the National Academy of Sciences*, vol. 104, no. 12, pp. 4984–4989, 2007.

[37] S. Eshghi, M. Khouzani, S. Sarkar, and S. Venkatesh, "Optimal patching in clustered epidemics of malware," *IEEE Trans. Network*, 2015.

[38] L. Yang, X. Yang, and Y. Wu, "The impact of patch forwarding on the prevalence of computer virus: A theoretical assessment approach," *Applied Mathematical Modelling*, vol. 43, pp. 110–125, 2017.

[39] D. Kempe, J. Kleinberg, and É. Tardos, "Maximizing the spread of influence through a social network," in *Proceedings of the ninth ACM SIGKDD international conference on Knowledge discovery and data mining*. ACM, 2003, pp. 137–146.

[40] L. Lü, D. Chen, X.-L. Ren, Q.-M. Zhang, Y.-C. Zhang, and T. Zhou, "Vital nodes identification in complex networks," *Physics Reports*, vol. 650, pp. 1–63, 2016.

[41] D. E. Knuth, *The Stanford GraphBase: a platform for combinatorial computing*. Addison-Wesley Reading, 1993, vol. 37.

[42] D. Lusseau and M. E. Newman, "Identifying the role that animals play in their social networks," *Proceedings of the Royal Society of London B: Biological Sciences*, vol. 271, no. Suppl 6, pp. S477–S481, 2004.

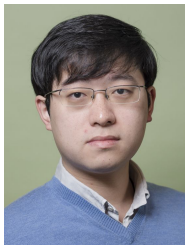

Zhidong He is pursuing his Ph.D. degree since September 2015 at Delft University of Technology, The Netherlands. He obtained his B.Sc. degree in School of Electronic Information and Electrical Engineering at Shanghai Jiao Tong University in 2011, and received his M.Sc. degree in College of Control Science and Engineering at Zhejiang University in 2014. His research interests include network science, epidemic dynamics, and wireless networks.

Piet Van Mieghem received the Masters (*magna cum laude*, 1987) and PhD (*summa cum laude*, 1991) degrees in electrical engineering from the K.U. Leuven, Leuven, Belgium. He is a Professor at the Delft University of Technology and Chairman of the section Network Architectures and Services (NAS) since 1998. His main research interests lie in modeling and analysis of complex networks and in new Internet-like architectures and algorithms for future communications networks. Before joining Delft, he worked at the Interuniversity Micro Electronic Center (IMEC) from 1987 to 1991. During 1993-1998, he was a member of the Alcatel Corporate Research Center in Antwerp, Belgium. He was a visiting scientist at MIT (1992-1993), a visiting professor at UCLA (2005), a visiting professor at Cornell University (2009), and at Stanford University (2015). He is the author of four books: Performance Analysis of Communications Networks and Systems (Cambridge Univ. Press, 2006), Data Communications Networking (Techne, 2011), Graph Spectra for Complex Networks (Cambridge Univ. Press, 2011), and Performance Analysis of Complex Networks and Systems (Cambridge Univ. Press, 2014).